Available online at www.sciencedirect.com
SCIENCE DIRECT®
Journal of Sound and Vibration 273 (2004) 515–542
JOURNAL OF SOUND AND VIBRATION
www.elsevier.com/locate/jsvi

Acoustical analysis of multiple cavities connected by necks in series with a consideration of evanescent waves

J.W. Lee[a,*], J.M. Lee[a], S.H. Kim[b]

[a] *Machine Dynamics Laboratory (301-215), School of Mechanical and Aerospace Engineering, Seoul National University, San 56-1, Shillim-dong, Kwanak-gu, Seoul 151-742, South Korea*
[b] *Division of Mechanical Engineering and Mechatronics, Kangwon National University, Chooncheon 200-701 Kangwon Do, South Korea*

Received 6 September 2002; accepted 28 April 2003

Abstract

In this paper, a new analytical method was developed to obtain the natural frequencies and natural modes of multiple cavities connected by necks or slits in series, which strongly affect the longitudinal acoustic modes. At the interface between a cavity and a neck, discontinuity in the cross-sectional area generates an evanescent wave in addition to a plane wave. The evanescent wave with a set of cross-modes decays along a distance from the neck, but the evanescent wave forces length correction term to be added to the characteristic equation of the enclosure. Therefore, the effective length, instead of the physical length of the neck, is used in the characteristic equation. We examined the validity of the proposed method by using finite element analysis for five cases. We also investigated the effect of changing the neck's position on the acoustical characteristics and the relation between added length and natural frequency.

1. Introduction

Modal properties of the enclosing structure and its interior cavity are important in determining the frequency response characteristics of a coupled structural–acoustic system. To reduce system noise, researchers have modified the structure of the enclosing body [1–4]. Some have enhanced acoustical characteristics by changing geometry and boundary conditions of the cavity, which determine acoustic modes [5,6]. In many cases, after a system is designed, its dimensions cannot be easily changed. If an acoustic system consists of several cavities connected by necks or slits, the design of necks or slits strongly affects the acoustical characteristics of the system. For example, a

*Corresponding author. Tel.: +82-2-880-7152; fax: +82-2-876-9493.
E-mail address: jw062@mailvib.snu.ac.kr (J.W. Lee).

0022-460X/03/$ - see front matter
doi:10.1016/S0022-460X(03)00508-X

vehicle compartment with a trunk can be regarded as the double cavities connected through holes on the package tray. Also, in a hard disk drive system, disks divide the internal cavity of the drive into several sub-cavities. Since acoustical modal characteristics of the multiple cavities dominate the acoustic response of the system, it is important to predict the natural frequencies and natural modes of the acoustic system in the design stage.

Many researchers have studied the acoustical modal characteristics of multiply-connected cavities. Dowell [7] derived formulas that determine acoustic natural frequencies of multiply-connected cavities by using the normal modes of the rigid-walled cavity. Morse and Ingard [8] used the Green function approach to obtain the same formulas for natural frequencies. They regarded the connecting hole as a pure opening with zero mass and stiffness and neglected the evanescent wave near the interface. We, however, consider the effect of evanescent wave as an important factor. Fahy and Schofield [9] studied the effect of a Helmholtz resonator on a large enclosure. They used the effective length of a neck, but it was not defined explicitly. Britz and Pollard [10] developed a method to find the natural frequencies of the Helmholtz resonator and enclosure system. They assumed that significant coupling occurs only between resonator modes and enclosure modes, which have close frequencies. Doria [11,12] studied the acoustical behavior of an enclosure connected to multiple resonators.

In similar studies, other researchers developed equations for the internal and external end correction to calculate the resonance frequency of a Helmholtz resonator. Ingard discussed some properties of a resonator in a free field or in a wall in regard to scattering and absorption of an incident plane wave [13,14]. Selamet [15–17] investigated the effect of specific cavity dimensions of resonators theoretically and experimentally. Panton and Miller [18] presented a simple but useful equation including the length correction term for cylindrical resonators. This equation is valid over a much larger range of wavelengths than the classic equation was. Chanaud [19,20] reported the influence of geometry on the resonance frequency of Helmholtz resonator. Although he also suggested that all the cross-modes and the plane wave are necessary for an exact calculation, he did not explicitly describe the effect of the cross-modes. Pollack [21] derived the axisymmetric limit of the inertial end correction for a pipe intersecting a plenum that is radially finite and axially infinite.

The present study proposes a theoretical method for natural frequencies of multiple rectangular cavities connected by necks or slits in series. First, we consider the effect of evanescent wave to derive a characteristic equation that determines the exact natural frequencies of a rectangular parallelepiped cavity with discontinuity in the cross-sectional area. Second, we compare our results by the proposed approach with the numerical values by the finite element analysis for five cases. Third, we investigate the effects of the cross-sectional area and the position of a neck on the natural frequencies of longitudinal acoustic modes. We also examine the relation between added length, which is created by evanescent wave, and natural frequency.

2. Theoretical formulation

The acoustic system we investigate has discontinuity in the cross-section. The discontinuity generates evanescent wave near the interface [19–21]. The evanescent wave with a set of cross-modes exists only around the interface and decays along a distance from the neck; however, it

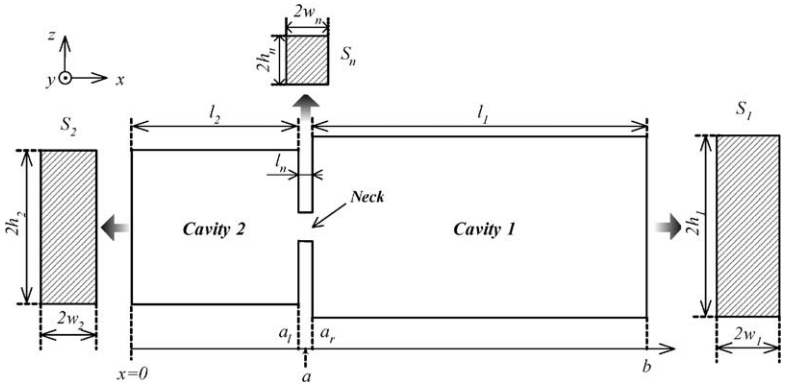

Fig. 1. Double cavities connected by a neck.

affects the natural frequency and local acoustic pressure distribution around the interface. This wave is considered in our work of deriving the characteristic equation for longitudinal acoustic modes and their natural frequencies.

Fig. 1 shows the acoustic enclosure, which consists of three parts. A neck, whose length is very small compared to the cavity length, connects two cavities. It has a cross-sectional area of S_n ($= 2w_n \times 2h_n$) and length of l_n. S_1 and S_2 are the cross-sectional areas of the two cavities, whose lengths, widths and heights are denoted by l_i, $2w_i$ and $2h_i$, respectively, where i is 1,2. x, y and z are rectangular co-ordinates defining a position in the acoustic enclosure.

Before we develop basic equations, we present several assumptions for our analysis. The first assumption is that length of each cavity is so large that all evanescent modes decay: $l_i > \max(2w_i, 2h_i)$. The length of the neck, however, is much smaller than the wavelength of sound, so the fluid in a neck can be regarded as a lumped mass element: $kl_n \ll 1$, $kw_n \ll 1$ and $kh_n \ll 1$, where k is the wave number. Also, the frequency considered in our analysis remains below the cut-on frequency of the first non-planar mode of all the cavities. It is because x-axial acoustic modes of our analytical model are more strongly affected by a neck connecting two cavities than other acoustic modes in a lower frequency range, but, at higher frequencies, cross-modes are generated by the neck and are affected as much as or much more than the x-axial modes. In conclusion, acoustic modes composed of standing wave in the x direction and evanescent wave with a set of cross-modes will be considered when validating the proposed method.

2.1. Basic equations

The homogeneous wave equation and the linearized Euler equation are expressed by

$$\nabla^2 \tilde{p} = \frac{1}{c^2}\frac{\partial^2 \tilde{p}}{\partial t^2}, \quad \tilde{p} = \tilde{p}(x, y, z, t), \tag{1}$$

$$-\nabla \tilde{p} = \rho \frac{\partial \tilde{u}}{\partial t}, \quad \tilde{u} = \tilde{u}(x, y, z, t), \tag{2}$$

where $\tilde{p}$ is the acoustic pressure, $\tilde{u}$ is the velocity fluctuation, c is the sound velocity, t is the time and ρ is the density of the acoustic medium.

And the acoustic pressure and velocity may be written as Eqs. (3) and (4) on the assumption of harmonic motion for the acoustic variables:

$$\tilde{p}(x,y,z,t) = p(x,y,z)\mathrm{e}^{\mathrm{j}\omega t}, \tag{3}$$

$$\tilde{u}(x,y,z,t) = u(x,y,z)\mathrm{e}^{\mathrm{j}\omega t}, \tag{4}$$

where ω is the angular frequency and $\mathrm{j} = \sqrt{-1}$.

In the rectangular cavity, appropriate solution of the wave equation (1) can be described by

$$\tilde{p}(x,y,z,t) = p(x,y,z)\mathrm{e}^{\mathrm{j}\omega t} = X(x)G(y,z)\mathrm{e}^{\mathrm{j}\omega t}. \tag{5}$$

Separation of variables results in the following set of equations:

$$\left(\frac{\mathrm{d}^2}{\mathrm{d}x^2} + k_x^2\right)X(x) = 0, \tag{6}$$

$$\left(\frac{\partial^2}{\partial y^2} + \frac{\partial^2}{\partial z^2} + k_{qs}^2\right)G(y,z) = 0, \tag{7}$$

where the separation constants are related by

$$k_x^2 + k_{qs}^2 = k^2 = (\omega/c)^2. \tag{8}$$

When the length of cavity is much longer than its height and width, the standing wave $\tilde{p}^s$ mainly in the x direction exists in the low-frequency range and can be described by

$$\tilde{p}^s(x,t) = p^s(x)\mathrm{e}^{\mathrm{j}\omega t} = (\tilde{A}\mathrm{e}^{\mathrm{j}k_x x} + \tilde{B}\mathrm{e}^{-\mathrm{j}k_x x})\mathrm{e}^{\mathrm{j}\omega t}, \tag{9}$$

where the constants $\tilde{A}$ and $\tilde{B}$ are determined by boundary conditions, and k_x is a pure real value and equal to k when no standing wave exists in the other direction. Also, when the sign of k_x^2 is negative, Eq. (1) has another solution, which represents the evanescent wave $\tilde{p}^e$ with a set of cross-modes. $\tilde{p}^e$ is expressed as follows:

$$\tilde{p}^e(x,y,z,t) = p^e(x,y,z)\mathrm{e}^{\mathrm{j}\omega t} = \sum_q \sum_s (C_{qs}\mathrm{e}^{-\alpha_{x_{qs}}x} + D_{qs}\mathrm{e}^{\alpha_{x_{qs}}x}) \cdot \Xi_{qs}(y,z)\mathrm{e}^{\mathrm{j}\omega t}, \tag{10}$$

where $\alpha_{x_{qs}} = -\mathrm{j}k_x = \sqrt{k_{qs}^2 - k^2}$ and the constants C_{qs} and D_{qs} depend on the boundary conditions. Also, $\Xi_{qs}(y,z)$ represents a cross-mode and is determined by the boundary conditions in the y and z directions. Note that one of two terms on the right-hand side of Eq. (10) can be removed depending on physical conditions.

Only Eq. (9) needs to be used to describe the acoustic pressure distribution in a long rectangular cavity without a hole, but Eq. (10) also needs to be considered to determine the acoustic mode in a long rectangular cavity with a hole. And the particle velocity $\tilde{u}$ is composed of the velocity $\tilde{u}^s$ related to the standing wave and the velocity $\tilde{u}^e$ related to the evanescent wave.

Harmonic motion of the fluid in the neck produces propagating wave $\tilde{p}^s$ and evanescent wave $\tilde{p}^e$. The forward-travelling wave interacts with the backward-travelling wave so that the propagating wave can form a standing wave. An evanescent wave contains a set of cross-modes and exists locally around the interface between the cavity and the neck, as shown in Fig. 2. A cavity with a neck on its left has evanescent wave decaying in the positive x direction and the evanescent wave of a cavity with a neck on its right decays in the negative x direction (see

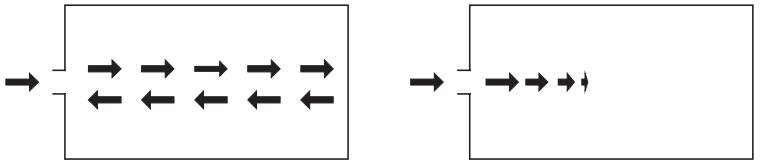

(a) Standing wave (b) Evanescent wave

Fig. 2. Standing wave and evanescent wave generated by a neck.

Eq. (10)). Hence, the acoustic pressure distribution of acoustic modes in each cavity is determined by the standing wave and the evanescent wave:

$$\tilde{p}_1(x,y,z,t) = (p_1^s(x) + p_1^e(x,y,z))\mathrm{e}^{\mathrm{j}\omega t},$$

$$\tilde{p}_2(x,y,z,t) = (p_2^s(x) + p_2^e(x,y,z))\mathrm{e}^{\mathrm{j}\omega t}, \tag{11}$$

where subscript 1 and 2 represent the cavity numbers, respectively. The evanescent waves, which was written as Eq. (10), of each cavity can be expressed as follows:

$$p_1^e(x,y,z) = \sum_{q=0}\sum_{s=0} M_{qs}\cos_1 k_q(y-w_1)\cos_1 k_s(z-h_1)\mathrm{e}^{-{}_1\alpha_{x_{qs}}(x-a_r)},$$

$$p_2^e(x,y,z) = \sum_{q=0}\sum_{s=0} N_{qs}\cos_2 k_q(y-w_2)\cos_2 k_s(z-h_2)\mathrm{e}^{{}_2\alpha_{x_{qs}}(x-a_l)}. \tag{12}$$

In Eq. (12), ${}_i\alpha_{x_{qs}} = \sqrt{{}_ik_q^2 + {}_ik_s^2 - k^2}$, where ${}_ik_q$ and ${}_ik_s$ are the wave numbers in the y direction given by $q\pi/2w_i$ and in the z direction given by $s\pi/2h_i$, respectively. Also, M_{qs} and N_{qs}, where q and s are not zero at the same time, depend on boundary conditions.

The boundary conditions at the rigid wall in the enclosure are

$$\tilde{u}_2(0,y,z,t) = u_2(0,y,z)\mathrm{e}^{\mathrm{j}\omega t} = 0, \quad \tilde{u}_1(b,y,z,t) = u_1(b,y,z)\mathrm{e}^{\mathrm{j}\omega t} = 0. \tag{13}$$

The continuity of volume velocity requires that

$$\int_{-h_2}^{h_2}\int_{-w_2}^{w_2} \tilde{u}_2(a_l,y,z,t)\,\mathrm{d}y\,\mathrm{d}z = S_n\tilde{u}_n(a_l,t), \tag{14}$$

$$\int_{-h_1}^{h_{1_1}}\int_{-w_1}^{w_1} \tilde{u}_1(a_r,y,z,t)\,\mathrm{d}y\,\mathrm{d}z = S_n\tilde{u}_n(a_r,t), \tag{15}$$

where subscript n represents the neck.

Assuming that $kl_n \ll 1$, the equation of motion at $x = a$ becomes

$$\rho l_n S_n \frac{\mathrm{d}^2\tilde{\xi}_n(t)}{\mathrm{d}t^2} = \int_{-h_n}^{h_n}\int_{-w_n}^{w_n} \tilde{p}_2(a_l,y,z,t)\,\mathrm{d}y\,\mathrm{d}z - \int_{-h_n}^{h_n}\int_{-w_n}^{w_n} \tilde{p}_1(a_r,y,z,t)\,\mathrm{d}y\,\mathrm{d}z, \tag{16}$$

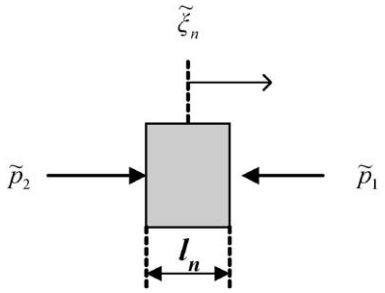

Fig. 3. Free body diagram of a lumped mass element in a neck.

where a is the middle point in the center axis of the neck and $\tilde{\xi}_n = \xi_n e^{j\omega t}$ is the displacement of a lumped mass element as shown in Fig. 3. Also, Eqs. (14) and (15) can be reduced to

$$S_2\tilde{u}_2^s(a_l,t) = S_n\frac{d\tilde{\xi}_n(t)}{dt} = S_1\tilde{u}_1^s(a_r,t). \tag{17}$$

2.2. Evanescent wave with a set of cross-modes

For convenience, evanescent wave near the interface between the neck and cavity 1 is considered first.

At $x = a_r$, continuity of velocity requires that

$$\tilde{u}_1(a_r,y,z,t) = u_1(a_r,y,z)e^{j\omega t} = \begin{cases} \dfrac{d\tilde{\xi}_n(t)}{dt}, & -w_n \leqslant y \leqslant w_n \text{ and } -h_n \leqslant z \leqslant h_n, \\ 0, & \text{otherwise.} \end{cases} \tag{18}$$

Using of orthogonality of trigonometric function from Eqs. (2) and (18), $p_1^e(x,y,z)$ is expressed as the function of the width ratio and the height ratio of the neck and the cavity 1. Also, it depends on the low order cross-modes, which have longer wavelengths, as shown in

$$p_i^e(x,y,z) = j\omega\rho(j\omega\xi_n)\sum_{q=0}\sum_{s=0}\frac{{}_i\phi_q\,{}_i\phi_s}{{}_i\alpha_{x_{qs}}}\cos_i k_q(y-w_i)\cos_i k_s(z-h_i)\,{}_iE_{qs}(x), \tag{19}$$

where ${}_iE_{qs}(x)$ becomes $e^{-{}_1\alpha_{qs}(x-a_r)}$ in the cavity 1 and $-e^{{}_2\alpha_{qs}(x-a_l)}$ in the cavity 2. And ${}_i\phi_q$ is the function of q, w_i and w_n, expressed by Eq. (20), and ${}_i\phi_s$ the function of s, h_i and h_n, expressed by Eq. (21):

$${}_i\phi_q = \int_{-w_n}^{w_n}\cos\left({}_ik_q(y-w_i)\right)dy \Big/ \int_{-w_i}^{w_i}\cos^2\left({}_ik_q(y-w_i)\right)dy, \tag{20}$$

$${}_i\phi_s = \int_{-h_n}^{h_n}\cos({}_ik_s(z-h_i))\,dz \Big/ \int_{-h_i}^{h_i}\cos^2({}_ik_s(z-h_i))\,dz, \tag{21}$$

where the preceding subscript i represents the cavity number.

If a neck is located at the center of the cross-section, symmetric cross-modes can be generated, but not antisymmetric cross-modes. The reason is that the symmetric cross-modes have non-zero volume displacement amplitude, but the volume displacement amplitude of antisymmetric cross-modes is zero [22]. So, the symmetric cross-mode of a lower order is easily generated and affects the natural frequencies.

2.3. Characteristic equation for the whole system

Substituting Eq. (11) into Eq. (16) results in

$$\begin{aligned} \mathrm{j}\omega\rho l_n S_n(\mathrm{j}\omega\xi_n) = &\left(\int_{-h_n}^{h_n}\int_{-w_n}^{w_n} p_2^s(a_l)\,\mathrm{d}y\,\mathrm{d}z + \int_{-h_n}^{h_n}\int_{-w_n}^{w_n} p_2^e(a_l,y,z)\,\mathrm{d}y\,\mathrm{d}z\right) \\ &- \left(\int_{-h_n}^{h_n}\int_{-w_n}^{w_n} p_1^s(a_r)\,\mathrm{d}y\,\mathrm{d}z\right. \\ &\left. + \int_{-h_n}^{h_n}\int_{-w_n}^{w_n} p_1^e(a_r,y,z)\,\mathrm{d}y\,\mathrm{d}z\right) \end{aligned} \tag{22}$$

And considering Eq. (17), Eq. (22) can be transformed as follows:

$$\begin{aligned} &\mathrm{j}\omega\rho\left(l_n + \frac{\int_{-h_n}^{h_n}\int_{-w_n}^{w_n} p_1^e(a_r,y,z)\,\mathrm{d}y\,\mathrm{d}z}{\mathrm{j}\omega\rho(\mathrm{j}\omega\xi_n)S_n} - \frac{\int_{-h_n}^{h_n}\int_{-w_n}^{w_n} p_2^e(a_l,y,z)\,\mathrm{d}y\,\mathrm{d}z}{\mathrm{j}\omega\rho(\mathrm{j}\omega\xi_n)S_n}\right) \\ &= -\frac{S_n p_1^s a_r)}{S_1 u_1^s(a_r)} + \frac{S_n p_2^s(a_l)}{S_2 u_2^s(a_l)}. \end{aligned} \tag{23}$$

The characteristic equation expressed by Eq. (24) is obtained from Eqs. (19) and (23):

$$\frac{kl_n'}{S_n} = \frac{\cot(kl_1)}{S_1} + \frac{\cot(kl_2)}{S_2}, \tag{24}$$

where the effective length l_n' of a neck is composed of the real length of the neck l_n and the added length Δl_n, which is created by the evanescent wave: $l_n' = l_n + \Delta l_n = l_n + \Delta l_1 + \Delta l_2$.

$$\Delta l_i = \frac{S_i}{S_n}\sum_{q=0}\sum_{s=0}\frac{1}{{}_i\alpha_{x_{qs}}}\,{}_i\varepsilon_{qs}\,{}_i\phi_q^2\,{}_i\phi_s^2, \quad {}_i\varepsilon_{qs} = \begin{cases} 1, & q\neq 0 \text{ and } s\neq 0, \\ 2, & \text{otherwise.} \end{cases} \tag{25}$$

Variables used in Eqs. (24) and (25) are expressed in non-dimensional form for case studies:

$$\pi\Omega L_{n1}'\frac{1}{S_{n1}} = \cot(\pi\Omega) + \frac{1}{S_{21}}\cot(\pi\Omega L_{21}), \tag{26}$$

$$\Delta L_{i1} = \frac{1}{S_{ni}}\sum_{q=0}\sum_{s=0}\frac{1}{{}_i\alpha_{x_{qs}}l_1}\,{}_i\varepsilon_{qs}\,{}_i\phi_q^2\,{}_i\phi_s^2, \tag{27}$$

where $\Omega = kl_1/\pi$, $L_{n1}' = L_{n1} + \Delta L_{n1} = l_n'/l_1$, $L_{n1} = l_n/l_1$, $\Delta L_{n1} = \Delta L_{11} + \Delta L_{21}$, $\Delta L_{i1} = l_i/l_1$, $L_{21} = l_2/l_1$, $S_{ni} = S_n/S_i$ and $S_{21} = S_2/S_1$.

And acoustic pressure distributions $\bar{p}$ of each cavity and the neck are represented by:

$$\bar{p}_1(X, Y_1, Z_1) = \cos(\pi\Omega(X - B)) - \Omega\pi\frac{\sin(\pi\Omega)}{S_{n1}} \times \sum_{q=0}\sum_{s=0} \frac{{}_1\phi_q\,{}_1\phi_s}{{}_1\alpha_{x_{qs}} l_1} \cos\left(\frac{q}{2}\pi(Y_1 - 1)\right)\cos\left(\frac{s}{2}\pi(Z_1 - 1)\right) e^{-{}_1\alpha_{x_{qs}} l_1 (X - A_l)}, \quad (28)$$

$$\bar{p}_2(X, Y_2, Z_2) = -\frac{1}{S_{21}}\frac{\sin(\pi\Omega L_{21})}{\sin(\pi\Omega)}\cos(\pi\Omega X) + \Omega\pi\frac{\sin(\pi\Omega)}{S_{n1}}\sum_{q=0}\sum_{s=0} \frac{{}_2\phi_q\,{}_2\phi_s}{{}_2\alpha_{x_{qs}} l_1} \cos\left(\frac{q}{2}\pi(Y_2 - 1)\right)\cos\left(\frac{s}{2}\pi(Z_2 - 1)\right) e^{{}_2\alpha_{x_{qs}} l_1 (X - A_r)} \quad (29)$$

$$\bar{p}_n = \pi\Omega\frac{L_{n1}}{S_{n1}}\sin(\pi\Omega), \quad (30)$$

where $X = x/l_1$, $Y_1 = y/h_1$, $Y_2 = y/h_2$, $Z_1 = z/h_1$, $Z_2 = z/h_2$, $A_r = a_r/l_1$, $A_l = a_l/l_1$ and $B = b/l_1$.

The characteristic equation (26) is derived for double cavities connected by a neck, but our proposed method can be applied to some limit cases in which the length of a neck approaches 0 and the height of a neck is equal to that of one of the two cavities.

3. Case studies

Five case studies are presented to verify the proposed method and to investigate the effects of the cross-sectional area and the position of a neck on the natural frequencies. In each case, the theoretical natural frequencies are calculated by MATLAB and are compared with those obtained from finite element analysis (ANSYS5.5). To calculate the natural frequencies exactly, we used enough elements to represent the acoustic pressure distribution near the interface. However, to compute efficiently, the proposed method is applied to the analytical models with constant width, and two-dimensional finite element modeling is used: $W_{n1}(= w_n/w_1) = W_{21}(= w_2/w_1) = 1$. Length ratio between cavity 2 and cavity 1 is 0.34 for the first four case studies: $L_{21} = 0.34$. Also length of each cavity in five case studies is larger than six times height: $6 \times 2h_i < l_i$.

3.1. Case study I: double cavities connected by a neck

Case study I considered one main cavity (cavity 1) and one auxiliary cavity (cavity 2) connected by a neck. This case study represents a simplified model of the compartment cavity and trunk cavity connected through holes on the package tray. The height of cavity 1 is the same as that of cavity 2, but the neck's height varies in the range of 0.1 to 0.9: $W_{n1} = W_{21} = 1$, $H_{21}(= h_2/h_1) = 1$, $L_{21} = 0.34$ and $L_{n1} = 0.012$. The neck is located at the center of the cross-section of the two cavities as shown in Fig. 1.

Theoretical non-dimensional natural frequencies are calculated for necks with different heights. Table 1 compares the theoretical values with those by finite element analysis (FEA). Natural

Table 1
Comparison of non-dimensional natural frequencies by the proposed method with those by FEA: Case study I

	H_{n1}	0.1	0.3	0.5	0.7	0.9
Ω_1	FEA	0.576	0.668	0.708	0.729	0.737
	Theory (with ΔL_{n1})	0.576	0.663	0.705	0.728	0.741
	Theory (without ΔL_{n1})	0.712	0.735	0.739	0.741	0.746
Ω_2	FEA	1.147	1.269	1.366	1.436	1.469
	Theory (with ΔL_{n1})	1.147	1.259	1.352	1.425	1.471
	Theory (without ΔL_{n1})	1.375	1.450	1.466	1.474	1.478
Ω_3	FEA	2.061	2.109	2.155	2.194	2.213
	Theory (with ΔL_{n1})	2.061	2.106	2.150	2.193	2.224
	Theory (without ΔL_{n1})	2.166	2.210	2.221	2.226	2.229
Ω_4	FEA	2.979	2.976	2.971	2.967	2.962
	Theory (with ΔL_{n1})	2.981	2.983	2.984	2.985	2.985
	Theory (without ΔL_{n1})	2.985	2.985	2.985	2.985	2.985
Ω_5	FEA	3.126	3.270	3.449	3.619	3.684
	Theory (with ΔL_{n1})	3.125	3.253	3.406	3.580	3.695
	Theory (without ΔL_{n1})	3.522	3.664	3.692	3.704	3.710
Ω_6	FEA	4.028	4.053	4.121	4.285	4.415
	Theory (with ΔL_{n1})	4.027	4.049	4.092	4.197	4.385
	Theory (without ΔL_{n1})	4.202	4.356	4.401	4.422	4.434

Ω_i: Non-dimensional natural frequency, $i = 1, \ldots, 6$.

frequencies of the analysis considering added length are much closer to those by ANSYS, while those of the analysis neglecting the added length deviates from those by ANSYS. Also, it is revealed that each natural frequency increases with the height ratio. Fig. 4 shows the acoustic pressure distribution of each acoustic mode when the height of a neck is one-tenth of that of cavity 1: $H_{n1}(= h_n/h_1) = 0.1$. The acoustic pressure distribution of each mode differs from the standing wave for existence of the evanescent wave, especially near the neck. The results agreed well with those obtained from finite element analysis.

When the cross-sectional area of a neck is small, and the wavelength of frequency of interest is much larger than the dimensions of a total acoustic system, the acoustic system has acoustic modes that are strongly affected by evanescent wave. And in their acoustic pressure distribution, fluid in a neck can be regarded as a point source or a line source because the acoustic pressure distribution is very similar to the acoustic field built by a point or line source in an open field: spherical and cylindrical waves have their own wave characteristics in the near field but become so close to planar waves at a great distance from their sources [22].

The added length of the neck is given as the series expansion of cross-modes, but only several low order cross-modes participate in the added length terms. As shown in Fig. 5, non-dimensional one-sided added length ΔL_{11} increases with the number of the used cross-modes from 2 to 12, but

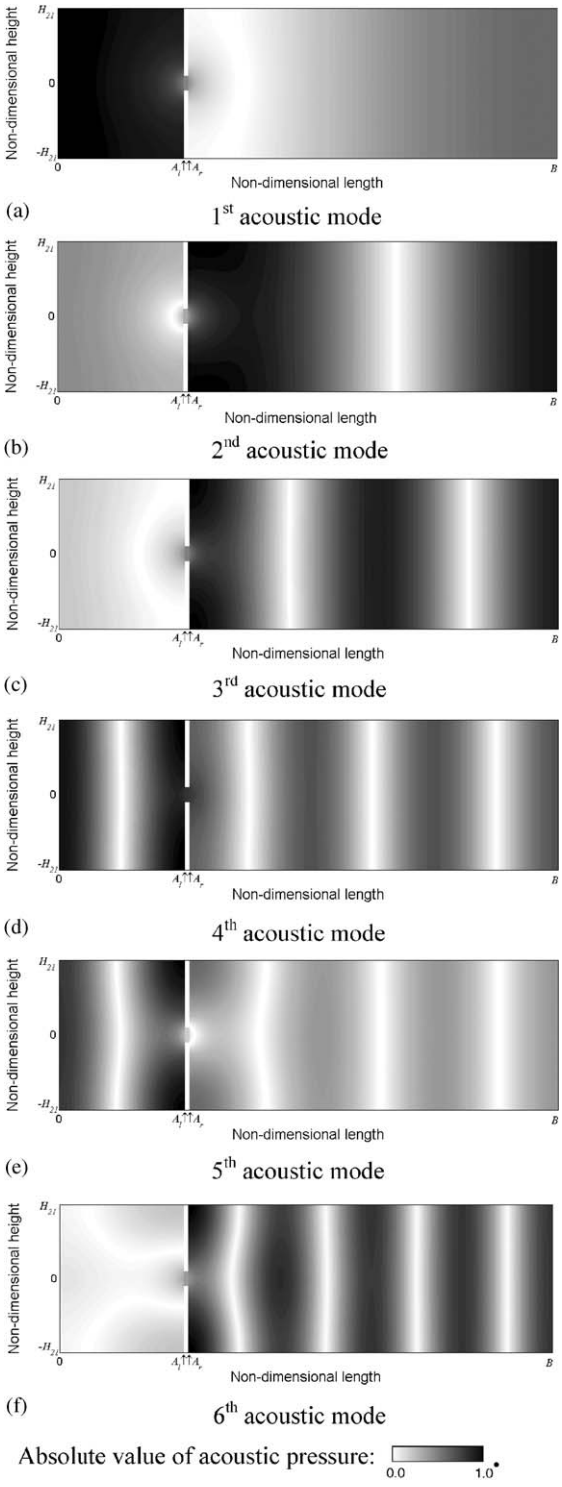

Fig. 4. Acoustic modes obtained by the proposed method (Case study I: $H_{n1} = 0.1$).

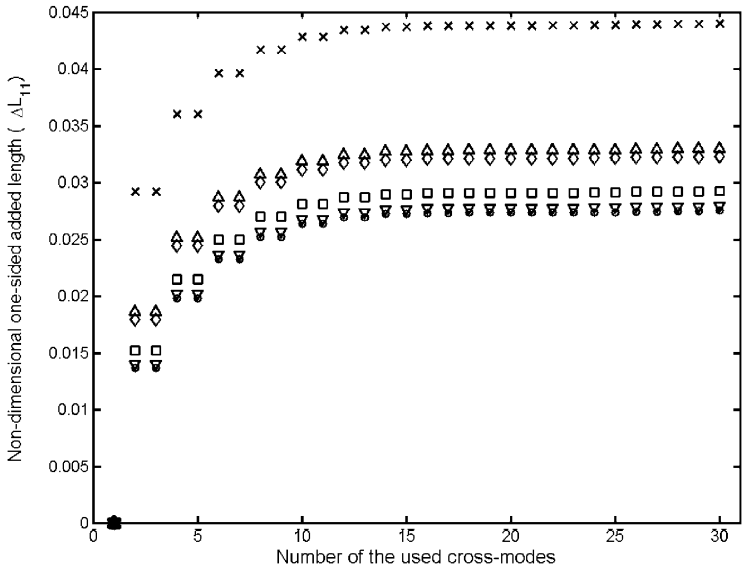

Fig. 5. Non-dimensional one-sided added length with the number of the used cross-modes ($H_{n1} = 0.1$), (○) 1st natural frequency, (▽) 2nd natural frequency, (□) 3rd natural frequency, (◇) 4th natural frequency, (△) 5th natural frequency, (×) 6th natural frequency.

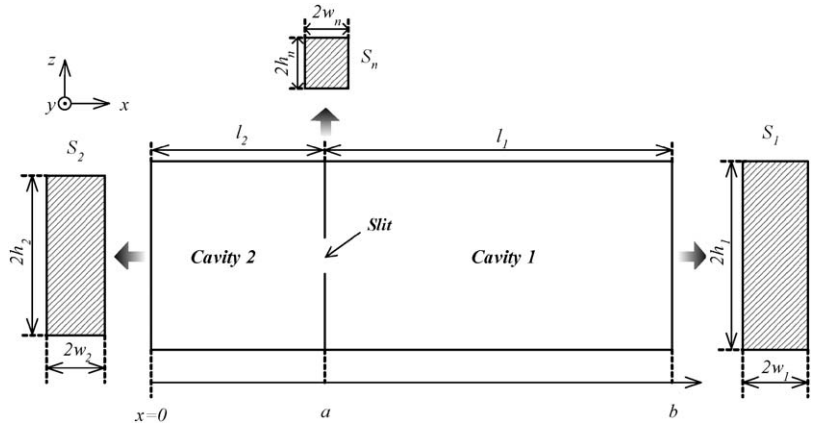

Fig. 6. Double cavities connected by a slit.

remains constant after 12, although the length can vary slightly depending on acoustic natural frequencies. Twelve cross-modes were used in this analysis.

3.2. Case study II: double cavities connected by a slit

In this section, our proposed method is applied to two sub-cavities connected by a slit. As shown in Fig. 6, the geometry used in this case study is the same as that of the previous section except $L_{n1} = 0$. Table 2 shows that the proposed method can calculate natural frequencies very

Table 2
Comparison of non-dimensional natural frequencies by the proposed method with those by FEA: Case study II

	H_{n1}	0.1	0.3	0.5	0.7	0.9
Ω_1	FEA	0.609	0.684	0.719	0.737	0.745
	Theory (with ΔL_{n1})	0.602	0.674	0.712	0.733	0.744
	Difference (%)	1.15	1.46	1.02	0.54	0.13
Ω_2	FEA	1.180	1.300	1.394	1.459	1.489
	Theory (with ΔL_{n1})	1.174	1.280	1.371	1.442	1.485
	Difference (%)	0.51	1.54	1.65	1.17	0.27
Ω_3	FEA	2.074	2.125	2.175	2.216	2.237
	Theory (with ΔL_{n1})	2.071	2.115	2.160	2.203	2.233
	Difference (%)	0.14	0.47	0.69	0.59	0.18
Ω_4	FEA	2.983	2.985	2.986	2.986	2.986
	Theory (with ΔL_{n1})	2.982	2.983	2.984	2.985	2.985
	Difference (%)	0.03	0.07	0.07	0.03	0.03
Ω_5	FEA	3.160	3.314	3.509	3.671	3.729
	Theory (with ΔL_{n1})	3.151	3.277	3.435	3.609	3.717
	Difference (%)	0.28	1.12	2.11	1.69	0.32
Ω_6	FEA	4.034	4.066	4.154	4.348	4.471
	Theory (with ΔL_{n1})	4.030	4.053	4.099	4.316	4.420
	Difference (%)	0.10	0.32	1.32	0.74	1.14

Ω_i: Non-dimensional natural frequency, $i = 1, \ldots, 6$. Difference (%) $= |\frac{\text{FEA} - \text{Theory with } \Delta L_{n1}}{\text{FEA}}| \times 100$.

close to those obtained from finite element analysis within a tolerance of 2.11 percent. Fig. 7 shows that acoustic pressure distribution of each mode is complex near the slit and that total acoustic pressure distribution seems to be created by a line source located at the interface.

3.3. Case study III: directly connected double cavities

The proposed method is applied to an acoustic system shown in Fig. 8, where two rectangular cavities with different cross-sectional areas are connected directly without a neck or a slit. This system can be considered an enclosure where the height of a neck is the same as that of cavity 2 and its length approximately zero: $H_{n1} = H_{21} < 1$, $L_{n1} = 0$, $L_{21} = 0.34$ and $W_{21} = 1$.

In this system, only cavity 1 has evanescent wave, but not cavity 2. The fact that $\Delta L_{11} \neq 0$ and $\Delta L_{21} = 0$ means that the evanescent wave can be generated only when the wave propagates from the small cross-section to the large cross-section (see Fig. 9). While the acoustic field in cavity 2 with a small cross-sectional area is composed of only standing wave, the acoustic pressure distribution in cavity 1 is composed of evanescent waves and standing wave. Table 3 shows that the non-dimensional natural frequencies of the theoretical model with the added length are much closer to those from FEA than those of the theoretical model without the added length.

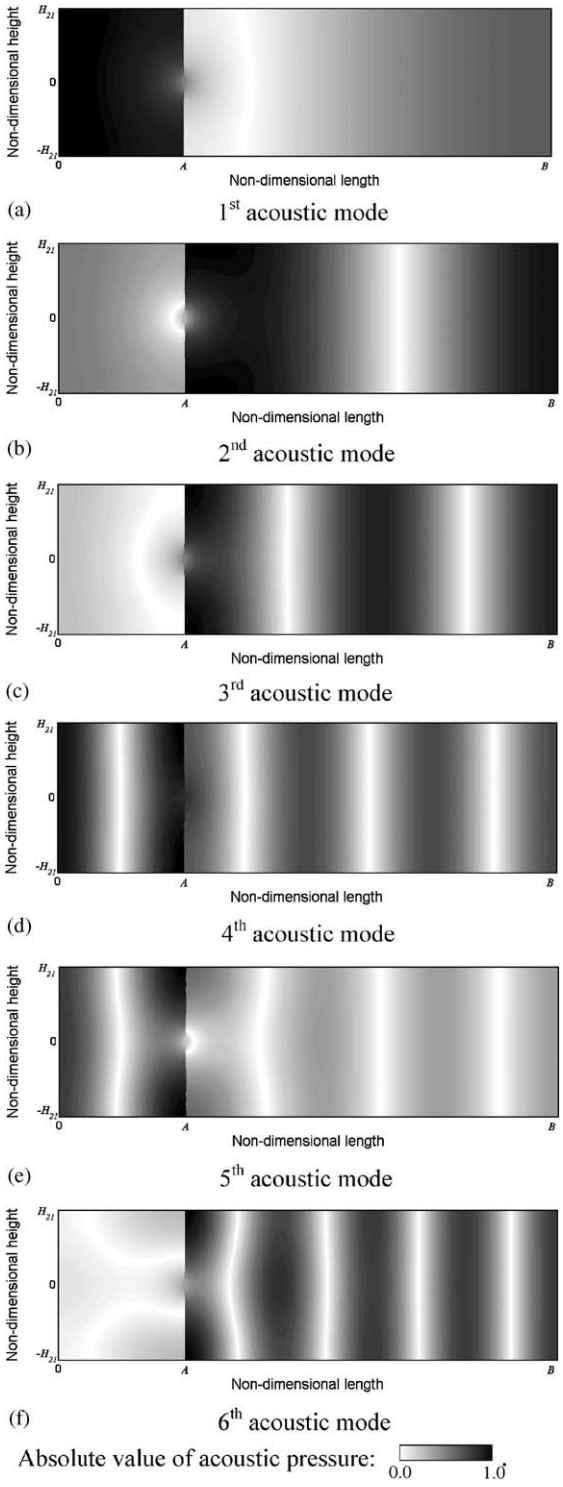

Fig. 7. Acoustic modes obtained by the proposed method (Case study II: $H_{n1} = 0.1$).

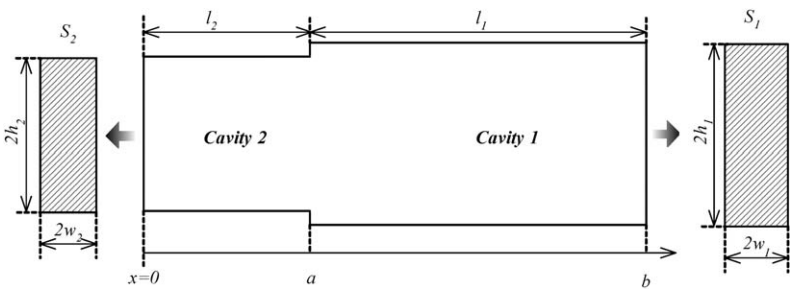

Fig. 8. Directly connected double cavities with different cross-sectional areas.

Especially, when $L_{21} = 0.5$ and $H_{21} = 0.5$, the theoretical model is the same as the model Dowell [7] used in his paper. Table 4 shows that the results obtained by our method and Dowell's agree qualitatively with those by finite element analysis.

3.4. Case study IV: the effect of the neck's position

In this section, the effect of the neck's position on the acoustic natural frequencies of an enclosure, as shown in Fig. 10, is investigated. This enclosure is the same as the system shown in Fig. 1 except that the position of a neck is changed and the height of the neck is one-tenth of that of cavity 1: $W_{21} = W_{n1} = 1$, $H_{21} = 1$, $H_{n1} = 0.1$, $L_{n1} = 0.012$ and $L_{21} = 0.34$. So, Eq. (21) is replaced by Eq. (31), and Eqs. (26) and (27) can be used again for this analysis:

$$ {}_i\phi_s = \int_{-h_n+g_n}^{h_n+g_n} \cos({}_ik_s(z-h_i))\,\mathrm{d}z \Big/ \int_{-h_i}^{h_i} \cos^2({}_ik_s(z-h_i))\,\mathrm{d}z, \tag{31} $$

where g_n is the distance between centers of the cavity and of the neck.

Table 5 shows that our proposed method can predict well the natural frequencies of the analytical model. If we neglect the added length created by the evanescent wave, we cannot explain the effect of the neck's position, which shall be discussed further in Section 4.2, on the acoustic natural frequencies.

3.5. Case study V: triple cavities connected by two necks in series and quadruple cavities connected by three necks in series

The proposed method is applied to three cavities connected by two necks in series and to four cavities connected by three necks in series, as shown in Fig. 11. All cavities have the same width and height, but different lengths. And the heights of the necks are one-tenth of the height of cavity 1; their lengths are twelve-thousandths (12/1000) of the length of the cavity 1; but their widths are equal to those of the cavities. The lengths of each cavity and each neck are denoted by l_i, where i is 1, 2, 3 and 4, and l_{n_i}, where i is 1, 2 and 3, respectively. Each neck is located at the centers of the cross-sections of the two adjoining cavities. Note that standing wave and evanescent wave exist in

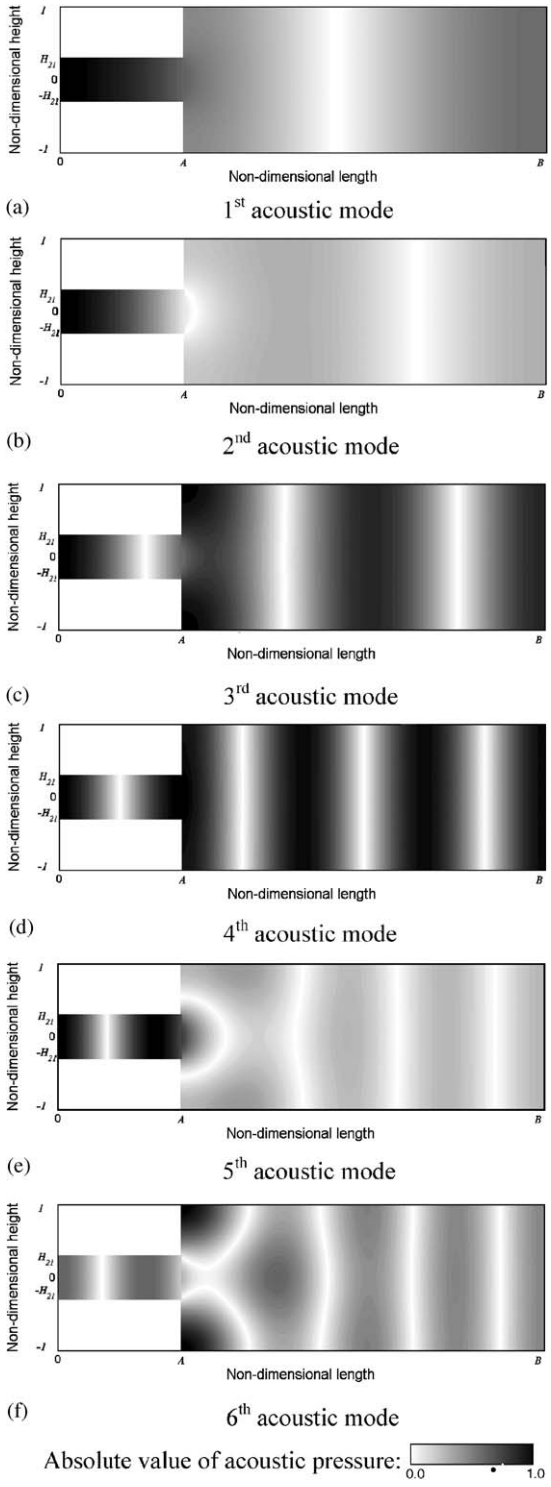

Fig. 9. Acoustic modes obtained by the proposed method (Case study III: $H_{21} = 0.3$).

Table 3
Comparison of non-dimensional natural frequencies by the proposed method with those by FEA: Case study III

	H_{21}	0.1	0.3	0.5	0.7	0.9
Ω_1	FEA	0.943	0.864	0.817	0.784	0.758
	Theory (with ΔL_{n1})	0.943	0.863	0.816	0.783	0.758
	Theory (without ΔL_{n1})	0.949	0.877	0.826	0.788	0.759
Ω_2	FEA	1.393	1.405	1.439	1.470	1.489
	Theory (with ΔL_{n1})	1.393	1.401	1.435	1.467	1.488
	Theory (without ΔL_{n1})	1.477	1.484	1.488	1.490	1.492
Ω_3	FEA	2.037	2.090	2.139	2.186	2.225
	Theory (with ΔL_{n1})	2.036	2.089	2.137	2.184	2.224
	Theory (without ΔL_{n1})	2.045	2.112	2.160	2.197	2.226
Ω_4	FEA	2.999	2.996	2.992	2.990	2.987
	Theory (with ΔL_{n1})	2.998	2.994	2.991	2.989	2.986
	Theory (without ΔL_{n1})	2.998	2.995	2.991	2.989	2.986
Ω_5	FEA	3.857	3.722	3.719	3.739	3.741
	Theory (with ΔL_{n1})	3.855	3.709	3.701	3.725	3.737
	Theory (without ΔL_{n1})	3.943	3.865	3.812	3.774	3.744
Ω_6	FEA	4.119	4.137	4.223	4.360	4.464
	Theory (with ΔL_{n1})	4.116	4.125	4.189	4.306	4.445
	Theory (without ΔL_{n1})	4.432	4.453	4.464	4.471	4.476

Ω_i: Non-dimensional natural frequency, $i = 1, \ldots, 6$.

Table 4
Comparison of non-dimensional natural frequencies by the proposed method, Dowell's results on the basis of results by FEA

	FEA	Dowell's		Proposed method
		Theory	Experiment	
Ω_1	0.718	0.71	0.72	0.718
Ω_2	1.245	1.22	1.24	1.243
Ω_3	2.000	2.02	2.00	2.000
Ω_4	2.671	2.65	2.62	2.663
Ω_5	3.200			3.192
Ω_6	4.003			4.000

Ω_i: Non-dimensional natural frequency, $i = 1, \ldots, 6$.

each cavity, and a cavity with necks on its both ends has two kinds of evanescent waves decaying in both directions (see Eq. (10)).

The same procedure used for double cavities connected by a neck is also applied to these two acoustic systems and the obtained results are summarized in Table 6: $l_2/l_1 = 0.56$, $l_3/l_1 = 0.34$ in

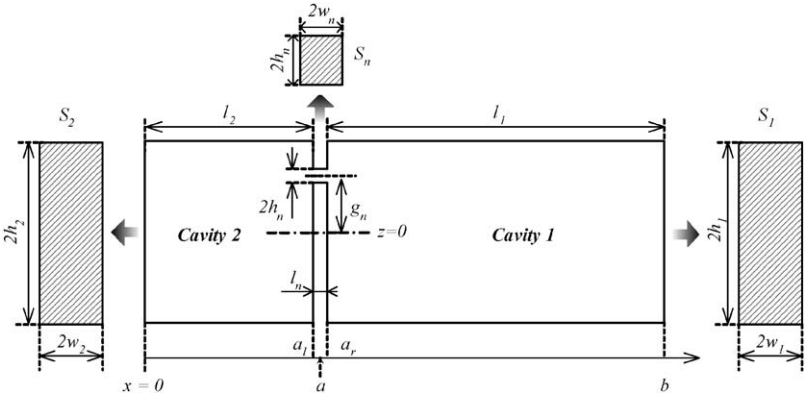

Fig. 10. Double cavities connected by a neck with a position change.

Table 5
Comparison of non-dimensional natural frequencies by the proposed method with those by FEA: Case study IV

	g_n/h_1	0	0.2	0.4	0.6	0.8
Ω_1	FEA	0.576	0.572	0.562	0.544	0.512
	Theory (with ΔL_{n1})	0.576	0.573	0.563	0.545	0.514
	Theory (without ΔL_{n1})	0.712	0.712	0.712	0.712	0.712
Ω_2	FEA	1.147	1.143	1.133	1.117	1.095
	Theory (with ΔL_{n1})	1.147	1.144	1.133	1.117	1.097
	Theory (without ΔL_{n1})	1.375	1.375	1.375	1.375	1.375
Ω_3	FEA	2.061	2.055	2.043	2.034	2.027
	Theory (with ΔL_{n1})	2.061	2.056	2.046	2.036	2.029
	Theory (without ΔL_{n1})	2.166	2.166	2.166	2.166	2.166
Ω_4	FEA	2.979	2.978	2.976	2.973	2.970
	Theory (with ΔL_{n1})	2.981	2.981	2.982	2.983	2.982
	Theory (without ΔL_{n1})	2.985	2.985	2.985	2.985	2.985
Ω_5	FEA	3.126	3.144	3.182	3.203	3.183
	Theory (with ΔL_{n1})	3.125	3.138	3.177	3.214	3.177
	Theory (without ΔL_{n1})	3.522	3.522	3.522	3.522	3.522
Ω_6	FEA	4.028	4.035	4.064	4.110	4.082
	Theory (with ΔL_{n1})	4.027	4.031	4.044	4.055	4.038
	Theory (without ΔL_{n1})	4.202	4.202	4.202	4.202	4.202

Ω_i: Non-dimensional natural frequency, $i = 1, \ldots, 6$.

the triple cavities connected by two necks and $l_2/l_1 = 0.78$, $l_3/l_1 = 0.56$ and $l_4/l_1 = 0.34$ in the quadruple cavities connected by three necks. The results reveal that the proposed method can also be applied to multiply connected cavities. Fig. 12 shows the acoustic pressure distribution of the triple cavities connected by two necks.

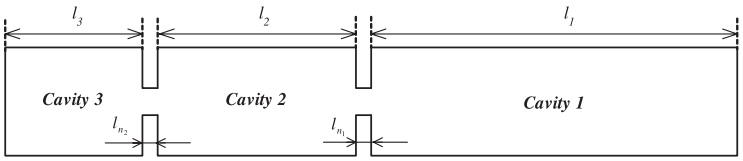

(a) Triple cavities connected by two necks in series

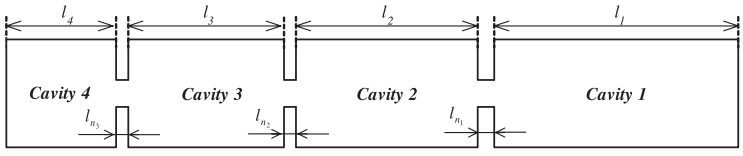

(b) Quadruple cavities connected by three necks in series

Fig. 11. Multiple cavities connected by necks in series.

Table 6
Comparison of non-dimensional natural frequencies of multiply connected cavities by the proposed method with those by FEA: Case study V

	Height ratio = 0.1	Three cavities with two necks	Four cavities with three necks
Ω_1	FEA	0.377	0.272
	Theory (With non-dimensional added length)	0.377	0.271
	Difference (%)	0.00	0.37
Ω_2	FEA	0.770	0.526
	Theory (With non-dimensional added length)	0.770	0.526
	Difference (%)	0.00	0.00
Ω_3	FEA	1.132	0.807
	Theory (With non-dimensional added length)	1.132	0.808
	Difference (%)	0.00	0.12
Ω_4	FEA	1.953	1.100
	Theory (With non-dimensional added length)	1.955	1.100
	Difference (%)	0.10	0.00
Ω_5	FEA	2.127	1.504
	Theory (With non-dimensional added length)	2.128	1.505
	Difference (%)	0.05	0.06
Ω_6	FEA	3.036	2.074
	Theory (With non-dimensional added length)	3.044	2.075
	Difference (%)	0.07	0.05

Ω_i: Non-dimensional natural frequency, $i = 1, \ldots, 6$. Difference (%) $= |\frac{\text{FEA}-\text{Theory}}{\text{FEA}}| \times 100$.

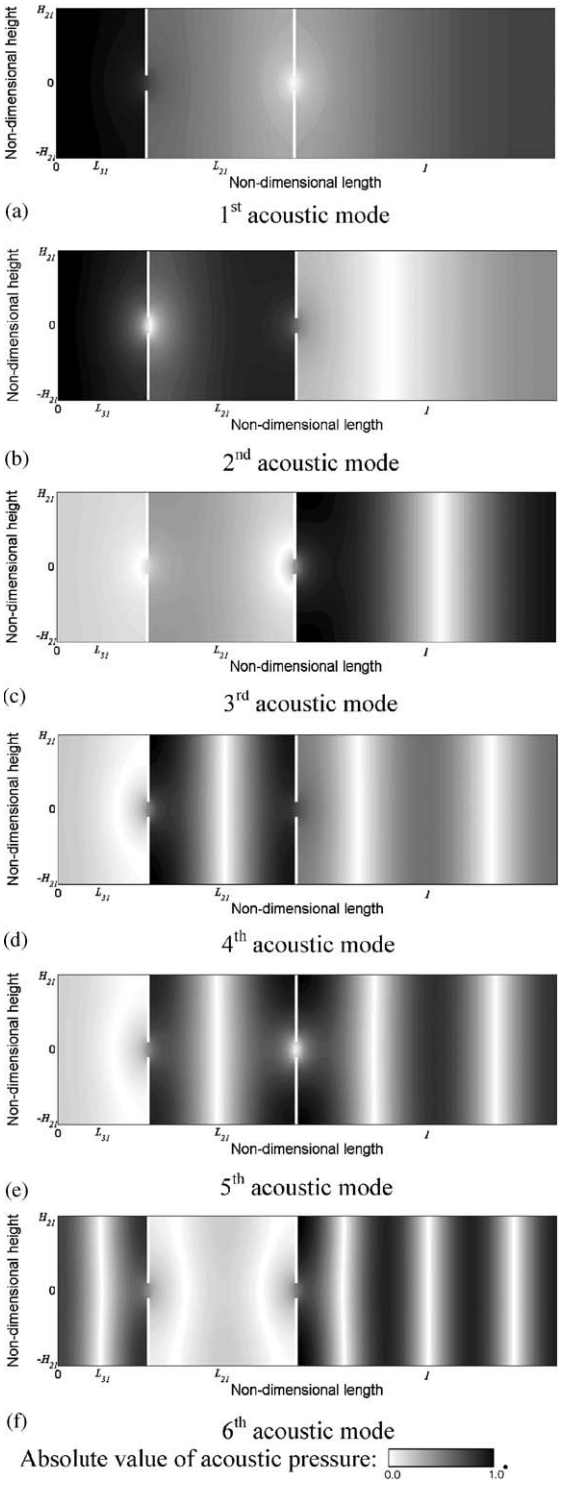

Fig. 12. Acoustic modes obtained by the proposed method (Case study V).

4. Discussion

4.1. Relation between the height ratio and the added length

The previous case studies support the consideration of added length in calculating natural frequencies of multiple cavities connected by necks or slits. Therefore, in this section, we investigate the relation between the non-dimensional added length and the height ratio on the basis of the results of Case study I.

From Eq. (25), one-sided added length (Δl_1) is created by evanescent wave with a set of cross-modes. These cross-modes are generated when a wave transmits from the small cross-section to the large cross-section. However, Fig. 5 shows that all cross-modes do not participate in the added length, but only several low order cross-modes participate in the added length, which affects the natural frequencies of an enclosure.

Also, non-dimensional one-sided added length varies with height ratio H_{n1} as shown in Fig. 13. It increases up to a ratio of about 0.3 and then decreases until the ratio becomes 1.0. This variation can be explained by the relation between non-dimensional one-sided added length ΔL_{11} and height ratio H_{n1} as shown in Eq. (32), which is obtained from Eqs. (21) and (27), and Eq. (33), which is derived from Eq. (32) through Taylor series:

$$\Delta L_{11} \propto \frac{1}{H_{n1}}\left[\frac{1}{s}\sin\left(\frac{s\pi}{2}H_{n1}\right)\right]^2, \tag{32}$$

$$\Delta L_{11} \propto \frac{1}{4}\pi^2 H_{n1} - \frac{s^2}{48}\pi^4 H_{n1}^3. \tag{33}$$

The variation of length is strongly affected by the first term on the right-hand side of Eq. (33) when H_{n1} is much less than 1. Therefore, it increases up to only a certain value and then decreases with the height ratio because it is governed by higher order terms with a minus sign. Fig. 13 shows the change of non-dimensional added length with the height ratio and its curve fitting using a third-order polynomial expressed by

$$\Delta L_{11} = \zeta_3 H_{n1}^3 + \zeta_2 H_{n1}^2 + \zeta_1 H_{n1}^1 + \zeta_0, \tag{34}$$

where these coefficients, shown in Table 7, are determined by least-squares method in MATLAB. The correlation coefficients (R-squared) evaluate the level of accuracy of the fit.

4.2. The effect of difference in position of a neck

Table 5 shows that enclosures with necks having the same cross-sectional area but located at different position have different natural frequencies. The reason is that non-dimensional added length of a neck varies with the neck's position as expressed by Eq. (35), which is derived from Eqs. (27) and (31). Eq. (35) can be approximated by a sixth-order polynomial expressed by Eq. (36):

$$\Delta L_{11} \propto \left[\cos\left(\frac{s\pi}{2}\left(\frac{g_n}{h_1} - 1\right)\right)\right]^2, \tag{35}$$

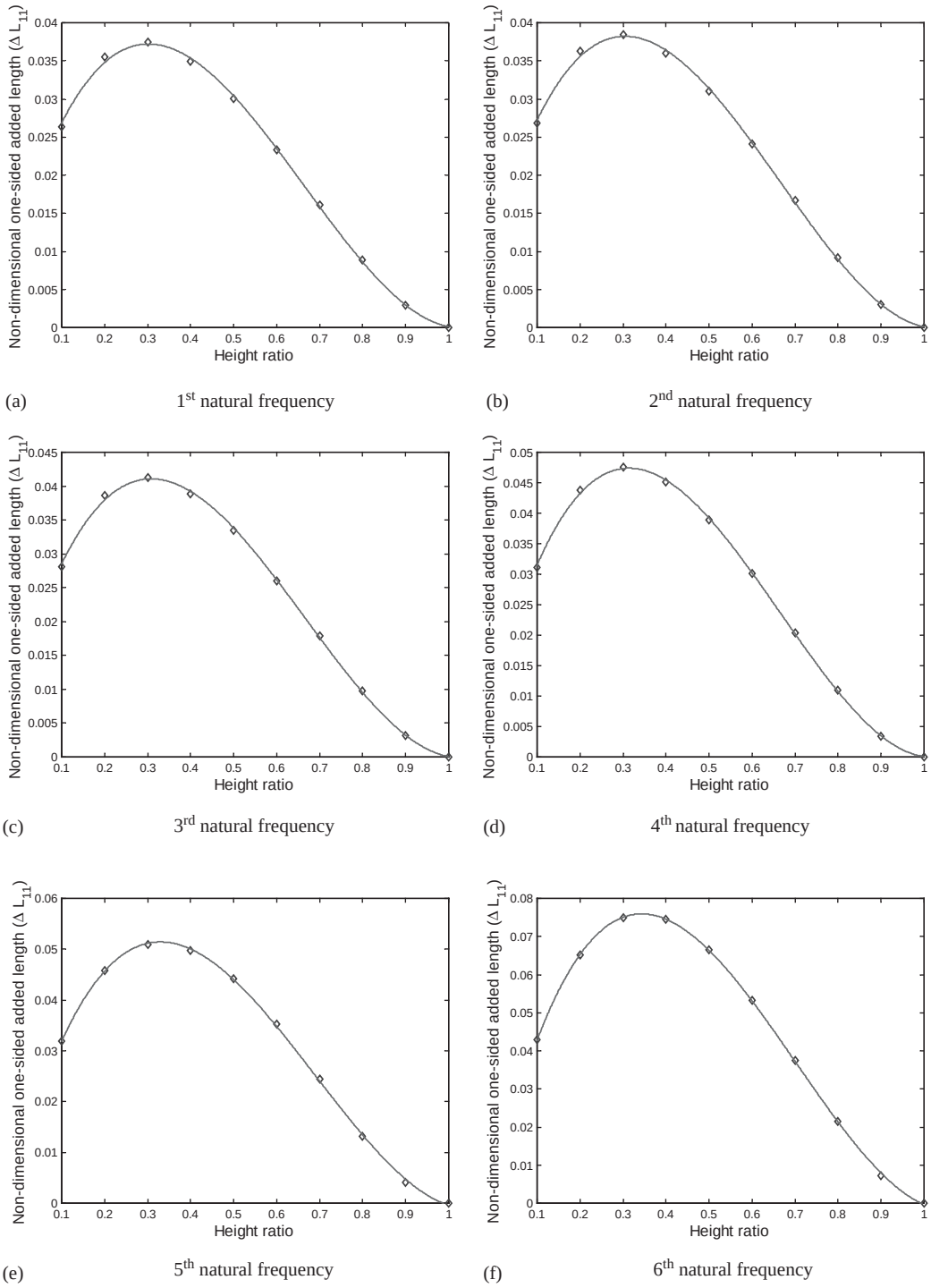

Fig. 13. Non-dimensional one-sided added length with the height ratio (from Case study I). (◇) calculated value, (—) curve fit.

Table 7
Coefficients and correlation (R-squared) value for curve fits based on Eq. (34)

Non-dimensional natural frequency	ζ_1	ζ_2	ζ_1	ζ_0	R^2
Ω_1	0.1967	−0.3918	0.1829	0.0123	0.9992
Ω_2	0.2034	−0.4064	0.1912	0.0120	0.9993
Ω_3	0.2246	−0.4490	0.2130	0.0115	0.9995
Ω_4	0.2739	−0.5465	0.2623	0.0104	0.9997
Ω_5	0.2829	−0.5852	0.2938	0.0081	0.9996
Ω_6	0.4256	−0.8950	0.4642	0.0048	0.9999

Ω_i: Non-dimensional natural frequency, $i = 1, \ldots, 6$.

Table 8
Coefficients and correlation (R-squared) value for curve fits based on Eq. (36)

Non-dimensional natural frequency	γ_6	γ_4	γ_2	γ_0	R^2
Ω_1	0.0535	−0.0310	0.0258	0.0260	0.9987
Ω_2	0.0536	−0.0342	0.0321	0.0264	0.9990
Ω_3	0.0678	−0.0910	0.1033	0.0278	0.9998
Ω_4	0.0074	0.0866	−0.0731	0.0307	0.9966
Ω_5	−0.0015	0.1003	−0.0784	0.0315	0.9972
Ω_6	−0.1130	0.2889	−0.1583	0.0423	0.9974

Ω_i: Non-dimensional natural frequency, $i = 1, \ldots, 6$.

$$\Delta L_{11} = \gamma_0 + \gamma_2 (g_n/h_1)^2 + \gamma_4 (g_n/h_1)^4 + \gamma_6 (g_n/h_1)^6. \tag{36}$$

The results of the curve fits are shown in Table 8, where the correlation coefficients (R-square) reveal that Eq. (36) can reasonably approximate the relation between the non-dimensional shift distance (g_n/h_1) and the non-dimensional one-sided added length (ΔL_{11}). The non-dimensional one-sided added length obtained from Eqs. (27) and (31) and fitted curves obtained from Eq. (36) are shown in Fig. 14 when the height ratio H_{n1} is 0.1.

Using Taylor series expressed by Eq. (37), Eq. (38) can approximate Eq. (26):

$$\cot(\beta x) \approx \frac{1}{\beta x} \quad \text{if } \beta x \ll 1, \tag{37}$$

$$\Omega \cong \frac{1}{\pi} \sqrt{\frac{H_{n1}}{L'_{n1}} \left(1 + \frac{1}{L_{21}} \frac{1}{H_{21}} \right)}. \tag{38}$$

The relation between the non-dimensional effective length and non-dimensional natural frequency can be described by

$$\Omega = \frac{\lambda_1}{\sqrt{L'_{n1}}} + \lambda_0, \tag{39}$$

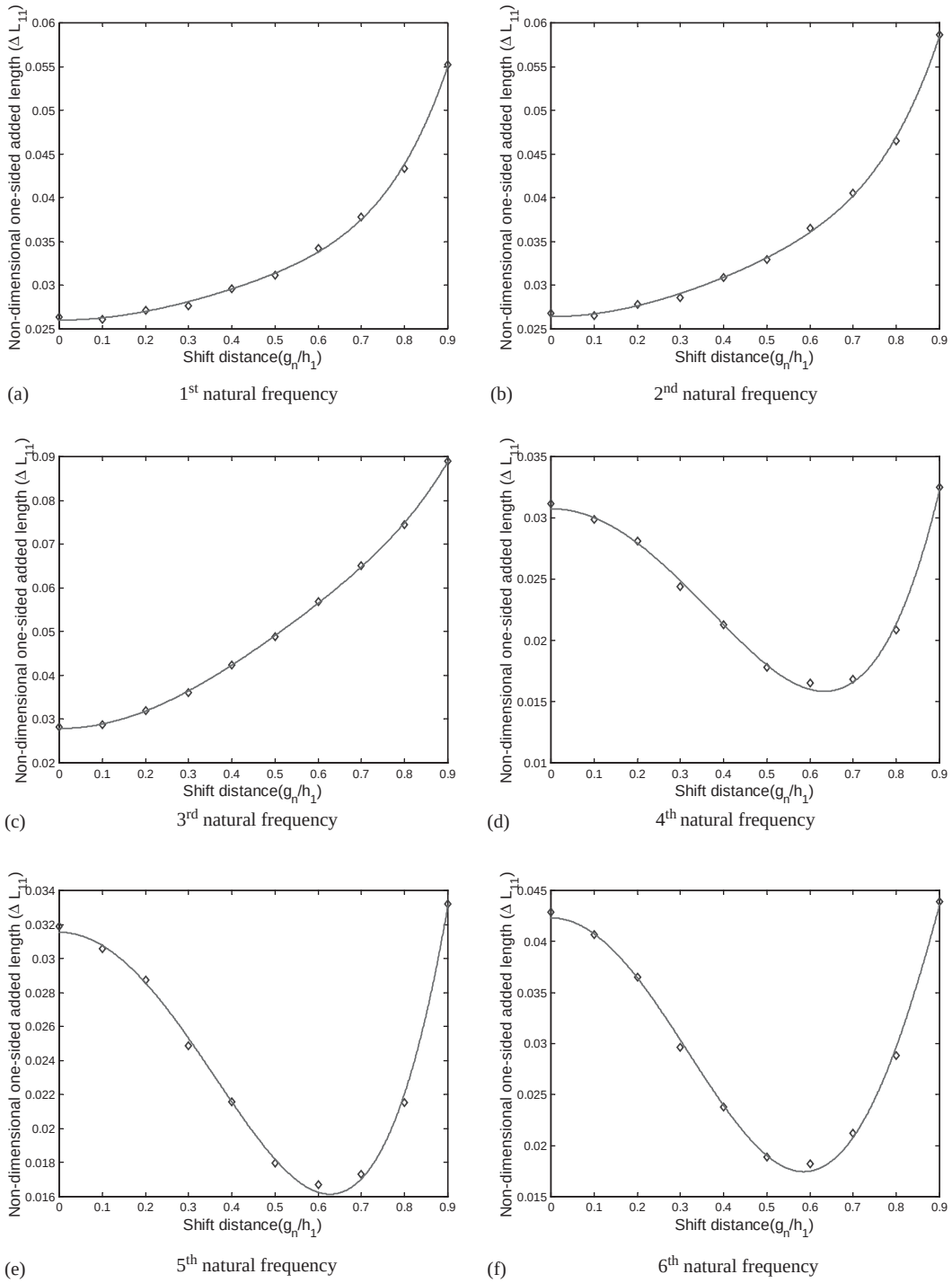

Fig. 14. Non-dimensional one-sided added length vs. non-dimensional shift distance of a neck. (◇) calculated value, (—) curve fit.

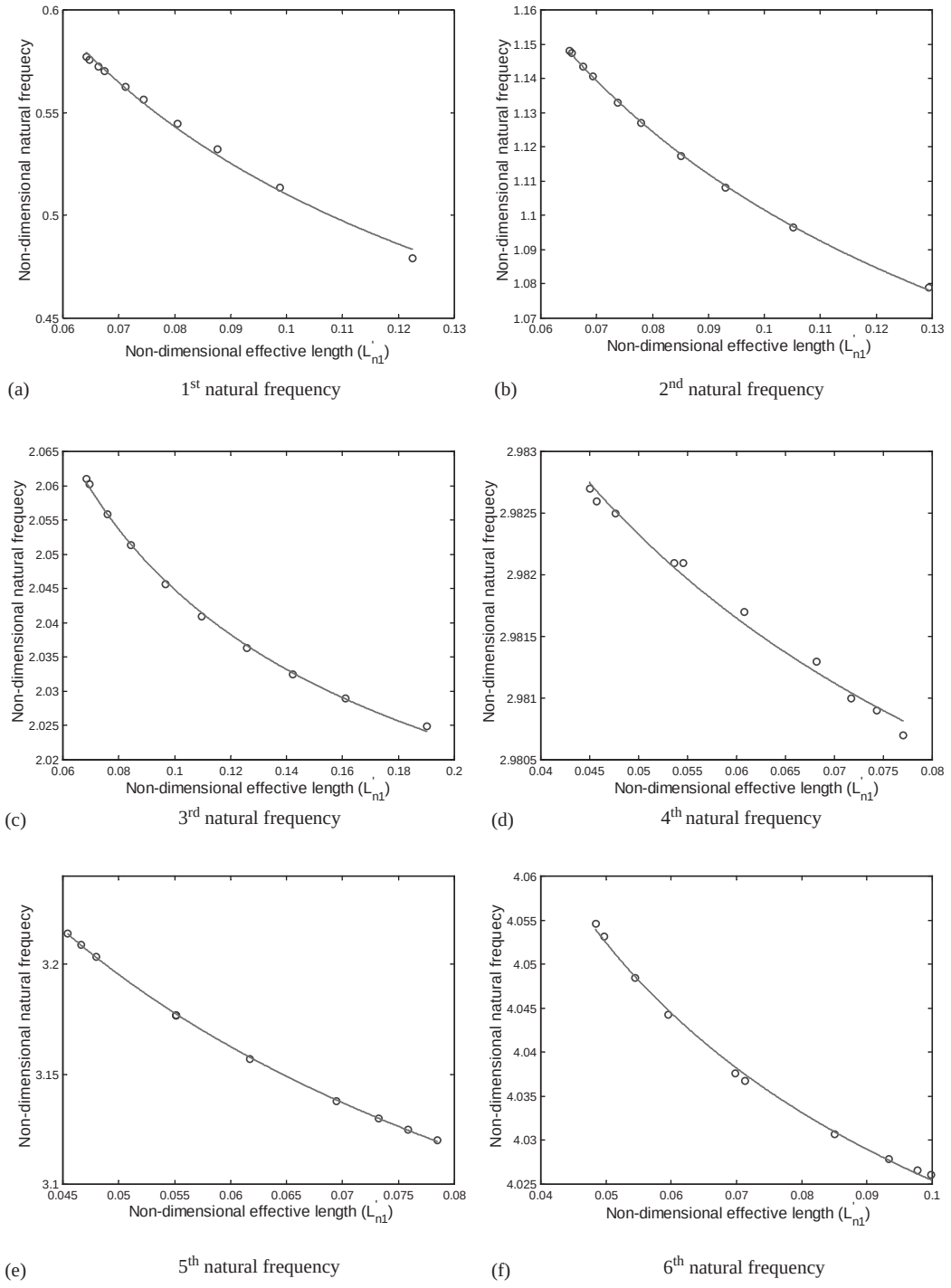

Fig. 15. Non-dimensional natural frequencies vs. non-dimensional effective length. (◦) calculated value, (—) curve fit.

Table 9
Coefficients and correlation (R-squared) value for curve fits based on Eq. (39)

Non-dimensional natural frequency	λ_1	λ_0	R^2
Ω_1	0.0880	0.2318	0.9948
Ω_2	0.0612	0.9080	0.9996
Ω_3	0.0238	1.9696	0.9991
Ω_4	0.0017	2.9745	0.9888
Ω_5	0.0840	2.8196	0.9998
Ω_6	0.0207	3.9601	0.9977

Ω_i: Non-dimensional natural frequency, $i = 1, \ldots, 6$.

where coefficients (λ_0, λ_1) are summarized with correlation coefficients in Table 9. Fig. 15 shows that natural frequencies of two cavities connected by a neck increase with the decreasing effective length.

5. Conclusions

In this paper, a useful method that can be used to calculate the natural frequencies of multiple cavities connected by necks or slits was presented. This method is not as complex as previous methods [7,8] in that no acoustic modes of each cavity alone are required. However, as the case studies revealed, the method did give natural frequencies that were closer to those obtained by the commercial FEA program (ANSYS 5.5). This fact was further supported when our results were compared with those obtained by the previous researcher [7].

Evanescent wave with a set of cross-modes generated by cross-sectional area expansion creates the added length. Therefore, we investigated the effects of different cross-sectional areas and of the neck's position on the natural frequencies. In addition, acoustic pressure distribution of each natural mode has also been studied. And the relation between non-dimensional effective length and non-dimensional natural frequency was discussed. By adjusting the cross-sectional area and position of a neck, we can obtain the enclosure with the desired characteristics.

We are currently studying the response of a coupled structural–acoustic system connected by necks or slits and will report the results.

Acknowledgements

This work was supported by the Brain Korea 21 project in 2002.

Appendix. Nomenclature

$\tilde{A}$, $\tilde{B}$	acoustic pressure amplitudes
S_{ni}	area ratio between a neck and the ith cavity

S_{21}	area ratio between cavities 2 and 1
A_r, A_l, B_0	non-dimensional points (a_r/l_1, a_l/l_1, b/l_1)
C_{qs}, D_{qs}, M_{qs}, N_{qs}	acoustic pressure amplitudes
c	sound velocity
$2h$	height of a cavity or a neck
H_{ni}	height ratio between a neck and the ith cavity
j	imaginary unit, $\sqrt{-1}$
k	wave number
k_x	wave number in the x direction
${}_ik_q$	wave number in the y direction of the ith cavity
${}_ik_s$	wave number in the z direction of the ith cavity
l	length of a cavity or a neck
l'_n	effective length of a neck
Δl_n	total added length of a neck
Δl_i	one-sided added length of a neck in the ith cavity
L_{n1}, L'_{n1}	non-dimensional length and effective length of a neck
L_{21}	non-dimensional length of the second cavity
ΔL_{n1}	non-dimensional added length
$\tilde{p}$	acoustic pressure
$\tilde{p}^e$	evanescent wave
$\tilde{p}^s$	standing wave
p	time-independent acoustic pressure
p^e	time-independent evanescent wave
p^s	time-independent standing wave
$\bar{p}_i$	non-dimensional acoustic pressure
S	cross-sectional area of a cavity or a neck
t	time
$\tilde{u}$	velocity fluctuation
u	time-independent velocity fluctuation
$2w$	width of a cavity or a neck
W_{ni}	width ratio between a neck and the ith cavity
X, Y_1, Y_2, Z_1, Z_2,	non-dimensional coordinates (x/l_1, y/h_1, y/h_2, z/h_1, z/h_2)

Greek letters

$\alpha_{x_{qs}}$	$-\mathrm{j}k_x = \sqrt{k_{qs}^2 - k^2}$
${}_i\alpha_{x_{qs}}$	$\sqrt{{}_ik_q^2 + {}_ik_s^2 - k^2}$
$\tilde{\xi}_n$	displacement of a lumped mass element in a neck
ω	angular frequency
$\Xi_{qs}(y,z)$	cross-mode
${}_iE_{qs}(x)$	exponential decay function of q, s and x
Ω	non-dimensional frequency ($= kl_1/\pi$)
ρ	density of the acoustic medium

Superscripts

e	evanescent wave
s	standing wave

Subscripts

i	number of a cavity
l, r	left and right of a specific point
n	a neck

References

[1] S.H. Kim, J.M. Lee, M.H. Sung, Structural–acoustic modal coupling analysis and application to noise reduction in a vehicle passenger compartment, *Journal of Sound and Vibration* 225 (5) (1999) 989–999.

[2] D.J. Nefske, J.A. Wolf Jr., L.J. Howell, Structural–acoustic finite element analysis of the automobile passenger compartment: a review of current practice, *Journal of Sound and Vibration* 80 (2) (1982) 247–266.

[3] S.H. Sung, D.J. Nefske, A coupled structural–acoustic finite element model for vehicle interior noise analysis, *American Society of Mechanical Engineers, Transactions, Journal of Vibration, Acoustics, Stress and Reliability* 106 (1984) 314–318.

[4] S.H. Kim, J.M. Lee, A practical method for noise reduction in a vehicle passenger compartment, *American Society of Mechanical Engineers, Journal of Vibration and Acoustics* 120 (1998) 199–205.

[5] S. Maruyama, A. Hasegawa, Y. Hyoudou, Interior noise analysis based upon acoustic excitation tests at low-frequency range, *SAE Proceedings of the 1999 Noise and Vibration Conference*, Vol. 2, Traverse City, MI, 1999, pp. 1203–1209.

[6] S.W. Kang, J.M. Lee, S.H. Kim, Structural–acoustic coupling analysis on vehicle passenger compartment with the roof, air-gap and trim boundary, *American Society of Mechanical Engineers, Journal of Vibration and Acoustics* 122 (3) (2000) 196–202.

[7] E.H. Dowell, G.F. Gorman III, D.A. Smith, Acoustoelasticity: general theory, acoustic natural modes and forced response to sinusoidal excitation, including comparisons with experiment, *Journal of Sound and Vibration* 52 (4) (1977) 519–542.

[8] P.M. Morse, K.U. Ingard, *Theoretical Acoustics*, McGraw-Hill Book Company, New York, 1968.

[9] F.J. Fahy, C. Schofield, A note on the interaction between a Helmholtz resonator and acoustic mode of an enclosure, *Journal of Sound and Vibration* 72 (3) (1980) 365–378.

[10] H.R. Britz, H.F. Pollard, Computational analysis of coupled resonators, *Journal Sound and Vibration* 60 (2) (1978) 305–307.

[11] A. Doria, Control of acoustic vibrations of an enclosure by means of multiple resonators, *Journal of Sound and Vibration* 181 (4) (1995) 673–685.

[12] A. Doria, A simple method for the analysis of Deep cavity and long neck acoustic resonators, *Journal of Sound and Vibration* 232 (4) (2000) 823–833.

[13] U. Ingard, On the theory and design of acoustic resonators, *Journal of the Acoustical Society of America* 25 (6) (1953) 1037–1061.

[14] U. Ingard, On the radiation of sound into a circular tube, with an application to resonators, *Journal of the Acoustical Society of America* 20 (5) (1948) 665–682.

[15] A. Selamet, P.M. Radavich, Helmholtz resonator: a multidimensional analytical, computational and experimental study, *SAE951263*, 1995, pp. 227–239.

[16] A. Selamet, N.S. Dickey, J.M. Novak, Theoretical, computational and experimental investigation of Helmholtz resonators with fixed volume: lumped versus distributed analysis, *Journal of Sound and Vibration* 187 (2) (1995) 358–367.

[17] N.S. Dickey, A. Selamet, Helmholtz resonators: one-dimensional limit for small cavity length-to-diameter ratios, *Journal of Sound and Vibration* 195 (3) (1996) 512–517.

[18] R.L. Panton, J.M. Miller, Resonant frequencies of cylindrical Helmholtz resonators, *Journal of the Acoustical Society of America* 57 (6Part II) (1975) 1533–1535.
[19] R.C. Chanaud, Effects of geometry on the resonance frequency of Helmholtz resonators, *Journal of Sound and Vibration* 178 (3) (1994) 337–348.
[20] R.C. Chanaud, Effects of geometry on the resonance frequency of Helmholtz resonators, part II, *Journal of Sound and Vibration* 204 (5) (1997) 829–834.
[21] M.L. Pollack, The acoustic inertial end correction, *Journal of Sound and Vibration* 67 (4) (1979) 558–661.
[22] L.E. Kinsler, A.R. Frey, A.B. Coppens, J.V. Sanders, *Fundamentals of Acoustics*, Wiley, New York, 1980.